

UCLA

UCLA Previously Published Works

Title

Brainstem Mechanisms of Pain Modulation: A within-Subjects 7T fMRI Study of Placebo Analgesic and Nocebo Hyperalgesic Responses.

Permalink

<https://escholarship.org/uc/item/0h592376>

Journal

Journal of Neuroscience, 41(47)

ISSN

0270-6474

Authors

Crawford, Lewis S

Mills, Emily P

Hanson, Theo

et al.

Publication Date






2021-11-24

DOI

10.1523/jneurosci.0806-21.2021

Peer reviewed

Brainstem Mechanisms of Pain Modulation: A within-Subjects 7T fMRI Study of Placebo Analgesic and Nocebo Hyperalgesic Responses

 Lewis S. Crawford,¹ Emily P. Mills,¹ Theo Hanson,¹  Paul M. Macey,² Rebecca Glarin,³
 Vaughan G. Macefield,^{4,5}  Kevin A. Keay,¹ and  Luke A. Henderson¹

¹School of Medical Sciences Neuroscience Program and Brain and Mind Centre, University of Sydney, New South Wales 2050, Australia, ²School of Nursing and Brain Research Institute, University of California, Los Angeles, Los Angeles, California 90095, ³Melbourne Brain Centre Imaging Unit, University of Melbourne, Melbourne, Victoria 3050, Australia, ⁴Baker Heart and Diabetes Institute, Melbourne, Victoria 3004, Australia, and ⁵Department of Anatomy and Physiology, University of Melbourne, Victoria 3050, Australia

Pain perception can be powerfully influenced by an individual's expectations and beliefs. Although the cortical circuitry responsible for pain modulation has been thoroughly investigated, the brainstem pathways involved in the modulatory phenomena of placebo analgesia and nocebo hyperalgesia remain to be directly addressed. This study used ultra-high-field 7 tesla functional MRI (fMRI) to accurately resolve differences in brainstem circuitry present during the generation of placebo analgesia and nocebo hyperalgesia in healthy human participants ($N = 25$, 12 male). Over 2 successive days, through blinded application of altered thermal stimuli, participants were deceptively conditioned to believe that two inert creams labeled lidocaine (placebo) and capsaicin (nocebo) were acting to modulate their pain relative to a third Vaseline (control) cream. In a subsequent test phase, fMRI image sets were collected while participants were given identical noxious stimuli to all three cream sites. Pain intensity ratings were collected and placebo and nocebo responses determined. Brainstem-specific fMRI analysis revealed altered activity in key pain modulatory nuclei, including a disparate recruitment of the periaqueductal gray (PAG)–rostral ventromedial medulla (RVM) pathway when both greater placebo and nocebo effects were observed. Additionally, we found that placebo and nocebo responses differentially activated the parabrachial nucleus but overlapped in engagement of the substantia nigra and locus coeruleus. These data reveal that placebo and nocebo effects are generated through differential engagement of the PAG–RVM pathway, which in concert with other brainstem sites likely influences the experience of pain by modulating activity at the level of the dorsal horn.

Key words: analgesia; hyperalgesia; nocebo; nociception; pain modulation; placebo

Significance Statement

Understanding endogenous pain modulatory mechanisms would support development of effective clinical treatment strategies for both acute and chronic pain. Specific brainstem nuclei have long been known to play a central role in nociceptive modulation; however, because of the small size and complex organization of the nuclei, previous neuroimaging efforts have been limited in directly identifying how these subcortical networks interact during the development of antinociceptive and pro-nociceptive effects. We used ultra-high-field fMRI to resolve brainstem structures and measure signal change during placebo analgesia and nocebo hyperalgesia. We define overlapping and disparate brainstem circuitry responsible for altering pain perception. These findings extend our understanding of the detailed organization and function of discrete brainstem nuclei involved in pain processing and modulation.

Received Apr. 14, 2021; revised Sep. 23, 2021; accepted Sep. 28, 2021.

Author contributions: L.S.C., E.P.M., K.A.K., and L.A.H. designed research; L.S.C., E.P.M., T.H., V.G.M., and L.A.H. performed research; P.M.M. and R.G. contributed unpublished reagents/analytic tools; L.S.C., T.H., and P.M.M. analyzed data; L.S.C. wrote the paper.

This work was supported by a research collaboration agreement with Siemens Healthineers. This work was also supported by the "NWG Macintosh Memorial Grant", obtained by the author E.P.M. We thank the facilities and the scientific and technical assistance of the Australian National Imaging Facility at the Melbourne Brain Centre Imaging Unit, University of Melbourne, and Assoc. Prof. Bradford Moffatt for developing the visual analog scale for use in the scanner.

The authors declare no competing financial interests.

Correspondence should be addressed to Luke A. Henderson at luke.henderson@sydney.edu.au.

<https://doi.org/10.1523/JNEUROSCI.0806-21.2021>

Copyright © 2021 the authors

Introduction

The perceived intensity of pain can be strongly influenced by expectations. For example, when an individual expects pain relief, an inert treatment can produce analgesic responses, that is, placebo analgesia. Conversely, if an individual expects pain intensification, an inert treatment can produce hyperalgesic responses, that is, nocebo hyperalgesia. These phenomena are thought to be mediated by descending neural pathways (Vanegas and Schaible, 2004; Eippert et al., 2009) originating within the cortex that are recruited in response to a combination of an

individual's expectations (Kirsch et al., 2014; Frisaldi et al., 2015; Egorova et al., 2019), conditioning effects (Voudouris et al., 1989, 1990; Medoff and Colloca, 2015; Babel et al., 2018), and environmental associations (Finniss et al., 2010; Hansen et al., 2017; Tinnermann et al., 2017). Although the phenomena of placebo analgesia and nocebo hyperalgesia are well documented, the basic circuitry underpinning their expression, in particular the circuits within the brainstem, remain largely undefined.

Given that expectation is critical for both placebo and nocebo responses, it is not surprising that human brain imaging investigations have reported changes in signal intensity during placebo and nocebo in higher brain regions including the prefrontal, cingulate, insular, and somatosensory cortices (Petrovic et al., 2002; Wager et al., 2004; Craggs et al., 2007; Frisaldi et al., 2015; Sevel et al., 2015; Schienle et al., 2018; Hibi et al., 2020; Schenk and Colloca, 2020). Additionally, there is evidence that these same higher brain regions recruit brainstem pain modulatory circuitry to mediate placebo and nocebo effects, most notably via a connection between the anterior cingulate cortex (ACC) and the periaqueductal gray (PAG), which is functionally altered during placebo (Wager et al., 2004; Bingel et al., 2006; Eippert et al., 2009) and nocebo (Tinnermann et al., 2017) responses.

Within the brainstem, the best described pain modulatory circuitry arises from neurons of the PAG, which project via a relay in the rostral ventromedial medulla (RVM) to neurons of the superficial dorsal horn (DH) of the spinal cord. Although some human brain imaging studies have reported signal change encompassing the PAG during experimental analgesic responses (Petrovic et al., 2002; Wager et al., 2004; Eippert et al., 2009; Grahl et al., 2018; Oliva et al., 2021), no study has accurately and robustly defined the complete brainstem circuits responsible for either placebo analgesic or nocebo hyperalgesic responses. Preclinical studies have established that opioid-mediated analgesic responses can be evoked from neurons in the ventrolateral column of the caudal PAG (vlPAG), whereas, a nonopioid analgesia can be triggered from neurons in the lateral PAG (lPAG) and dorsolateral PAG (dlPAG) columns (Bandler and Shipley, 1994; Coulombe et al., 2016; Sims-Williams et al., 2017).

As the administration of the opioid antagonist naloxone can attenuate placebo analgesia in humans (Amanzio and Benedetti, 1999; Eippert et al., 2009), it has been hypothesized that the vlPAG in particular plays a critical role in its expression. However, limited spatial acuity in previous imaging studies has prevented exact localization of signal changes within specific PAG columns, which raises doubt over whether within the human brainstem this phenomenon is potentiated by opioidergic projections that arise from the vlPAG. Additionally, depending on the method of conditioning, placebo analgesia has shown to be naloxone resistant (Vase et al., 2005; Benedetti et al., 2011), which suggests alternative brainstem systems outside of or including adjacent PAG columns may play a key role in the expression of placebo analgesia. Similarly, the question of whether specific PAG columns play a role in nocebo responses also remains to be addressed experimentally.

The development of ultra-high-field-strength (7 tesla) MRI has made precise identification of brainstem circuitry possible and provides the opportunity to resolve the PAG at a columnar level (Satpute et al., 2013). Indeed, 7 tesla investigations have already successfully identified specific patterns of PAG columnar recruitment during respiratory control (Faull et al., 2015) and shifting cognitive load (Kragel et al., 2019). Despite our understanding that pain modulatory circuits originating in the vlPAG

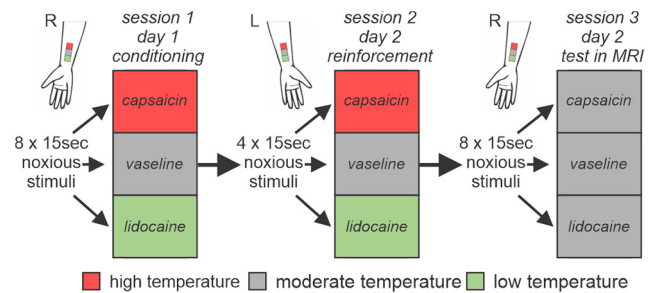


Figure 1. Experimental protocol. Conditioning and reinforcement were conducted by surreptitiously applying a series of individually calculated low-intensity thermal noxious stimuli to the lidocaine cream site, moderate intensity stimuli to the control cream site, and high intensity stimuli to the capsaicin cream site despite informing participants that all three cream sites were receiving identical intensity stimuli. An expectation of pain rating was collected before each series of stimuli as a measure of belief that the creams were acting to modulate participants' perceived pain. During the test phase, all three creams actually received identical moderate intensity thermal stimuli, and placebo and nocebo responsiveness were determined by calculating the difference in reported pain among the three cream sites.

are strongly modulated by opioids, whereas those originating in the dlPAG and lPAG are nonopioidergic (Palazzo et al., 2010; Linnman et al., 2012), no studies have been performed at 7 tesla to identify specific PAG columnar associations of placebo analgesia and nocebo hyperalgesia.

The aim of this study was to use ultra-high-field functional MRI (fMRI) to identify the brainstem circuitry mediating placebo analgesia and nocebo hyperalgesia in healthy humans. We hypothesized that placebo and nocebo responses would be characterized by different activation patterns and columnar recruitment of the PAG-RVM pathways and that each response would elicit significant signal changes in other key nuclei linked to pain modulation and perception.

Materials and Methods

Ethics

All experimental procedures were approved by the University of Sydney Human Research Ethics Committee and were consistent with the Declaration of Helsinki. Written informed consent was obtained from participants at the beginning of each session. Participants were also provided with an emergency buzzer while inside the scanner so that they could stop the experiment at any time. At the conclusion of testing, participants were informed both verbally and through a written statement of the necessary deception and true methodology of the experiment and were invited to seek clarification of what they had just experienced.

Participants

Twenty-seven healthy control participants were recruited for the study (13 male, 14 female; mean age, 22.7 ± 0.7 years \pm SEM; range, 19–33 years). To evaluate the necessary number of participants required for this study, an a priori power analysis (Faul et al., 2007) was performed using results from a previous imaging study investigating analgesic brainstem mechanisms (Youssef et al., 2016). This revealed a total sample size of 21 would be necessary to detect similar effect sizes with 95% power ($d = 0.84$, $\alpha = 0.05$, $power = 0.95$). Before beginning the study, participants completed a data sheet recording current medication(s) and any alcohol or caffeine ingested in the 24 h before testing.

Experimental design

The study included three sessions occurring on 2 successive days—a conditioning session on day 1, and a reinforcement and MRI scanning session on day 2 (Fig. 1). Throughout the study, noxious stimuli were administered to the volar surface of participants' left and right forearms using a 3×3 cm MR-compatible Peltier element thermode, which delivered a heat stimulus at a preprogrammed temperature via a Thermal

Sensory Analyzer (TSA-II, Medoc). Each stimulus lasted 15 s, including a ramp-up period (4° per second), a plateau period at a noxious temperature, and a ramp-down period (4° per second). Each stimulus was separated by a 15 s interstimulus-interval at a nonpainful baseline temperature of 32°C . Throughout conditioning, participants rated their pain on-line using a horizontal 10 cm visual analog scale (VAS) ranging between 0 and 100, where 0 was described as no pain and 100 as the worst pain imaginable. During scanning, participants used an MR-compatible button box to continuously report their pain perception. The VAS scale was shown on a reflected digital screen at the end of the magnet bore, and participants controlled the position of a slider to report their pain continuously by holding the left button (moved slider toward 0) or right button (moved slider toward 10) with their left middle and index fingers.

Day 1-conditioning protocol. Session 1 was conducted outside the MRI and consisted of two rounds of a conditioning protocol. Participants were first informed both verbally and via a written statement that the study was designed to investigate the modulatory effects of two active creams: a topical anesthetic containing lidocaine, which had been shown to provide pain relief in some individuals, and a hyperalgesic containing capsaicin, which had been shown to increase thermal sensitivity. A third cream was stated to be purely Vaseline and was described as a negative control to evaluate typical pain responses. In reality, all three creams contained purely Vaseline and only differed in color and their described properties. We then conducted a determination of moderate pain test, where 10 randomized stimuli ranging from 44 to 48.5°C in 0.5°C intervals were delivered to the volar aspect of the left forearm. Participants were informed that we were interested in recording a temperature that elicited a moderate subjective pain response (40 – 50 VAS rating) and that this temperature would be used throughout the remainder of the experiment. However, using the ratings provided during the determination of moderate pain, we delivered the following three different temperature stimuli: a low pain temperature (20 – 30 VAS rating), a moderate pain temperature (40 – 50 VAS rating), and a high pain temperature (60 – 70 VAS rating). These three temperatures were then deceptively applied to the different cream sites throughout the remainder of sessions 1 and 2.

Creams were then applied to three adjacent 3×3 cm squares on the volar surface of the participants' right forearm. To increase believability that the creams contained active substances, false labels were attached to the cream bottles, and green or red food coloring was added to the lidocaine and capsaicin creams, respectively. The Vaseline control cream always occupied the central square, and the green lidocaine and red capsaicin creams were counterbalanced between participants to occupy either the distal or proximal squares to reduce sensitivity effects. Ten minutes following cream application, we conducted two rounds of conditioning. Participants believed they would receive eight identical moderate thermal stimuli and were instructed to report their perceived pain intensity using the VAS. Participants were also asked before each set of stimuli for an average expectation of the pain they would experience, which acted both to measure belief that the creams were working to modulate their subjective pain and to reinforce the pain relieving and enhancing qualities of the creams. During the two conditioning rounds we deceptively applied a moderate temperature to the central control cream site, a low temperature to the green lidocaine cream site, and a high temperature to the red capsaicin cream site.

Day 2-reinforcement and test protocols. At approximately the same time on the following day, sessions 2 and 3 were conducted with participants inside the MRI machine and consisted of a reinforcement protocol (session 2) and a test protocol (session 3). The creams were applied to the volar surface of both left and right forearms, in the same order and locations as session 1, and once again described to hold powerful pain modulatory effects. Reinforcement was conducted by applying four noxious stimuli at the same low, middle, and high temperatures that were used throughout session 1 to the participants' left volar forearm. This reinforcement protocol was conducted to ensure that despite the change of day and immediate environment (inside the MRI), all participants continued to report different expectations and subjective pain across the three cream sites.

Following this reinforcement protocol, we waited 15 min for residual pain and sensitivity to dissipate before beginning the test protocol. During this 15 min period structural brain scans were collected. Unlike in sessions 1 and 2, the test protocol consisted of all three cream sites on the volar surface of the participant's right volar forearm receiving identical moderate intensity stimuli. We asked each participant for an average expectation of pain intensity directly before stimulation and instructed each participant to report the pain intensity experienced over the duration of the scan using the button box and the projected digital VAS. Each participant received four consecutive series of eight stimuli, with a separate functional series collected during each set of stimuli. The control cream site was always stimulated during the first and third series, and the lidocaine and capsaicin cream sites were stimulated during the second and fourth series, so that half of the participants received the placebo analgesia condition before the nocebo hyperalgesia condition, and the other half received a nocebo hyperalgesia condition before the placebo analgesia condition. This procedure ensured that each of the lidocaine and capsaicin stimulation periods were compared with an independent control cream site stimulation period. Furthermore, the counterbalanced condition presentation reduced the potential for order effects (Fig. 1).

fMRI data acquisition and preprocessing

Brain images were acquired using a whole-body Siemens MAGNETOM 7T MRI system with a combined single-channel transmit and 32-channel receive head coil (Nova Medical). Participants were positioned supine with their head in the coil and sponges supporting the head laterally to minimize movement. A T1-weighted anatomic image set covering the whole brain was collected (repetition time = 5000 ms, echo time = 3.1 ms, raw voxel size = $0.73 \times 0.73 \times 0.73$ mm, 224 sagittal slices, scan time = 7 min). The four fMRI acquisitions each consisted of a series of 134 gradient-echo echo-planar measurements using blood oxygen level-dependent (BOLD) contrast covering the entire brain. Images were acquired in an interleaved collection pattern with a multiband factor of four and an acceleration factor of three (repetition time = 2500 ms, echo time = 26 ms; raw voxel size = $1.0 \times 1.0 \times 1.2$ mm, 124 axial slices, scan time = 6 min and 25 s).

Image preprocessing and statistical analyses were performed using SPM12 (Penny et al., 2011) and custom software. Functional images were slice-time corrected, and the resulting six directional movement parameters were inspected to ensure that all fMRI scans had no more than 1 mm of linear movement or 0.5° of rotation movement in any direction. Images were then linearly detrended to remove global signal changes, and physiological noise relating to cardiac and respiratory frequency was removed using the DRIFTER toolbox (Särkkä et al., 2012), and the six-parameter movement-related signal changes were modeled and removed using a linear modeling of realignment parameters procedure. Using the spatially unbiased infratentorial template (SUIT) toolbox (Diedrichsen, 2006) for both the fMRI and T1 image sets, the brainstem and cerebellum were isolated and then normalized to the brainstem- and cerebellum-only template in Montreal Neurologic Institute (MNI) space. During this process, both the T1 structural and functional image sets were resliced into 0.5 mm isotropic voxels, and these images were spatially smoothed using a 1 mm full-width at-half maximum Gaussian filter. Data were upsampled, and a small smoothing kernel was applied to align with recommendations from Sclocco et al. (2018) to enhance the accurate investigation of signal intensity changes within small brainstem nuclei.

Placebo and nocebo responders versus nonresponders

Participants were grouped as either a responder or nonresponder separately for placebo and nocebo based on the 2 SDs method described previously by Youssef et al. (2016). Briefly, for the eight noxious stimuli delivered during the control (Vaseline) scan, the SD of the eight pain intensity ratings was calculated. During the subsequent lidocaine and capsaicin cream scans, the average pain intensity rating was calculated, and if this rating was either 2 SDs of the control average above for the capsaicin cream scan or 2 SDs below for the lidocaine cream scan, the participant was considered a responder. If not, the participant was considered a

nonresponder. Additionally, the average change in pain intensity ratings was also calculated for each participant during the lidocaine and capsaicin scans relative to the immediately previous control scan, which informed their placebo and nocebo ability, respectively. Significant differences between groups with respect to expected changes in pain intensities immediately before testing were determined using paired *t* tests (two tailed, $p < 0.05$). Because participants were grouped into either responder or nonresponder categories based on their perceived pain intensities during the fMRI scans (session 3), we did not assess significant differences between groups for the perceived pain intensity changes. A single-factor ANOVA ($p < 0.05$) was used to determine whether there were differences in the temperatures applied or pain intensity ratings reported between responder and nonresponder groups during the two control scans.

fMRI statistical analysis

To determine significant changes in signal intensity during each noxious stimulation period, a repeating boxcar model convolved with a canonical hemodynamic response function was applied to each of the four fMRI series. The first five volumes of each scan were removed from the model because of excessive signal saturation from the scanner. The contrast images generated for each functional image series were then used in group analyses.

We conducted three separate analyses to determine differences in brainstem activity during the placebo and nocebo responses, as well as the specific PAG columnar recruitment during these phenomena. In analysis 1, significant signal intensity changes within brainstem regions of responder and nonresponder groups were determined for both the lidocaine (placebo analgesia) and capsaicin (nocebo hyperalgesia) cream scans compared with the immediately preceding control (Vaseline) cream scans using random effects, paired voxel-by-voxel analyses. In analysis 2, significant relationships between regional brainstem activity changes (lidocaine–control β maps or capsaicin–control β maps) and the magnitude of placebo analgesic and nocebo hyperalgesic responses (mean pain intensity change relative to the control scan) were determined using random effects, voxel-by-voxel analyses. In analysis 3, PAG columnar and RVM rostrocaudal organization of placebo analgesic and nocebo hyperalgesic responses was explored. For the PAG, masks encompassing the dorsomedial (dmPAG), dlPAG, lPAG, and vlPAG columns as defined by Bandler and Keay (1996) were created at 1 mm intervals throughout the PAG's rostrocaudal extent (MNI *z* coordinates, -3 to -11) and for the RVM, dorsal (dRVM), middle (mRVM), and ventral (vRVM), masks were created at 1 mm intervals throughout the RVM's rostrocaudal extent ($z = -39$ to -51). The mean \pm SEM number of voxels in each mask at each rostrocaudal level were the following: vlPAG 18 ± 0 , lPAG 18 ± 0 , dlPAG 18 ± 0 , dmPAG 16 ± 0 , dRVM 126 ± 1 , mRVM 130 ± 10 , and vRVM 142 ± 11 . The number of 0.5 mm^3 voxels that were significantly positively or negatively correlated with either placebo or nocebo were then determined for each mask and plotted as a percentage of the total volume of each mask.

Analyses 1 and 2 were initially visualized at a threshold of $p < 0.005$, uncorrected with a cluster extent threshold of five contiguous voxels. Cluster-level correction for multiple comparisons was performed on resulting clusters ($p < 0.05$) to reduce the likelihood of type I errors. The locations of significant clusters in MNI space were tabulated, and β values extracted to determine the directions of signal changes. For display purposes, significant clusters were overlaid onto a mean T1-weighted anatomic of all 25 participants. So that the brainstem axial slices were aligned to the plane of standard human brainstem atlases (Paxinos and Huang, 2013), we altered the tilt of the display images so that the long axis of the brainstem was vertically oriented. This was achieved by tilting the overlays by 0.4 radians. The MNI coordinates of significant clusters were derived before this rotation.

Results

Psychophysics results

Data from two participants were excluded because of excessive variability in pain ratings during the test phase, which resulted in

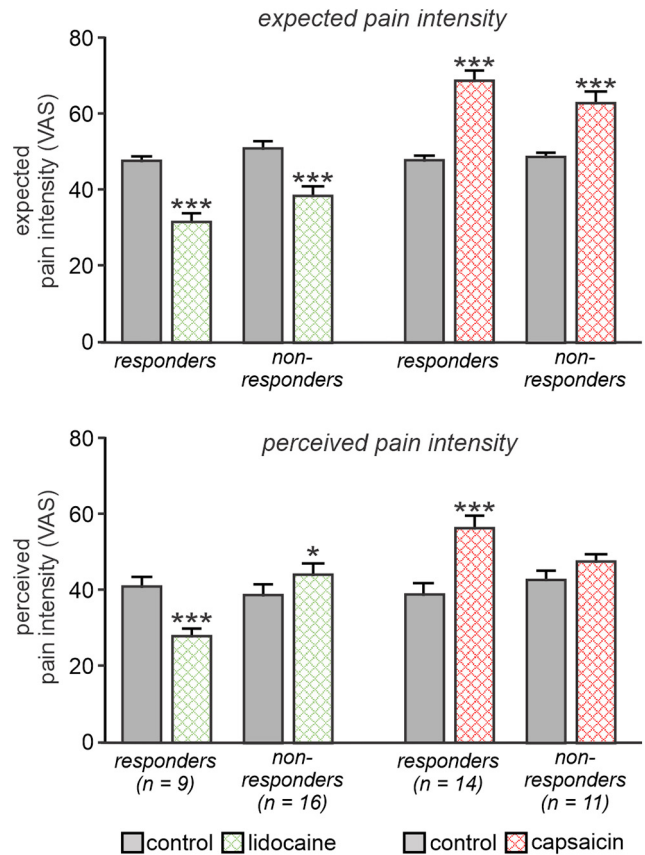


Figure 2. Expected and perceived pain intensities. Plots of mean (\pm SEM) expected pain intensity (top) and perceived pain intensity (bottom) during noxious stimuli delivered during the test phase. Note that both responder and nonresponder groups expected a pain reduction during stimulation of the lidocaine site and an increase during stimulation of the capsaicin site compared with stimulation of the control site. However, although responders' expectations were met by perceived pain intensity reductions or increases during actual stimulation of lidocaine and capsaicin sites, respectively, in the nonresponder groups expectation and perceived changes in pain were not met. That is, nonresponder groups did not experience a modulatory response to match their expectations and reported similar pain across the three cream sites. * $p < 0.05$, *** $p < 0.001$.

ceiling and floor effects and consequently an inability to accurately measure placebo analgesic or nocebo hyperalgesic effects. Data from 25 participants were included in the final psychophysical and functional image analyses. For the placebo analgesia protocol, 9 participants were classified as responders (36%) and 16 as nonresponders (64%), and for the nocebo hyperalgesia protocol 14 participants were classified as responders (56%) and 11 as nonresponders (44%). Of the 25 participants tested, six were categorized as both placebo and nocebo responders, and eight as both placebo and nocebo nonresponders.

Participants' expectations of pain directly before each of the test scans revealed that all four groups expected the creams to significantly alter pain intensity (Fig. 2). That is, both placebo responders and nonresponders expected their pain to be significantly inhibited during lidocaine cream stimulation compared with control (mean \pm SEM VAS responder: control 47.2 ± 1.4 , lidocaine 31.1 ± 2.5 ; nonresponder: control 50.4 ± 2.3 , lidocaine 38.1 ± 3.5 ; both $p < 0.001$). Likewise, both nocebo responders and nonresponders expected significantly enhanced pain during capsaicin cream stimulation compared with control (responder: control 48.3 ± 0.9 , capsaicin 68.3 ± 2.9 ; nonresponder: control 48.0 ± 1.9 , capsaicin 62.5 ± 3.1 ; both $p < 0.001$).

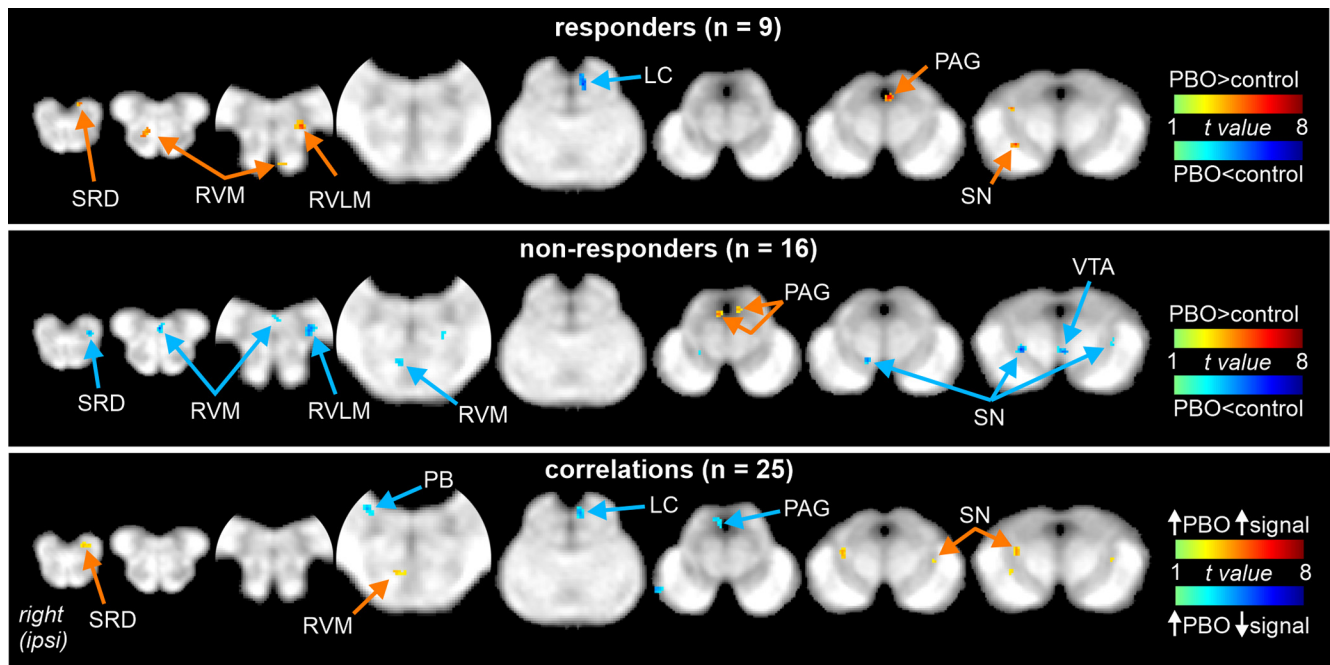


Figure 3. Signal changes in placebo responders, nonresponders, and sites where signal change correlated with placebo ability. Brainstem activity differed significantly between the control and lidocaine (placebo, PBO) scans in several pain modulatory nuclei. In responders (top), significant signal decreases (cool color scale) occurred in the region of the contralateral (to stimulation) LC, and signal increases (hot color scale) occurred in the ipsilateral SN, the contralateral ventrolateral PAG, RVL, SRD, and RVM. In nonresponders (middle), signal increases occurred in the PAG bilaterally, the contralateral RVL, the VTA and RVM. Signal intensity changes significantly correlated with placebo ability (bottom) were found to be positively correlated (hot color scale) in the SN bilaterally, the contralateral SRD, and RVM and negatively correlated (cool color scale) in the PAG, ipsilateral PB and contralateral LC. LC = locus coeruleus, SN = substantia nigra, PAG = periaqueductal gray, RVL = rostral ventrolateral medulla, SRD = subnucleus reticularis dorsalis, RVM = rostral ventromedial medulla.

In contrast, and consistent with the categorization of each participant, during actual stimulation of the lidocaine site, placebo responders reported reduced pain intensities compared with the preceding control site (Mean \pm SEM VAS control 40.7 ± 2.5 , lidocaine 27.3 ± 2.3), and placebo nonresponders reported an increase in pain intensity during stimulation on the lidocaine site (control 38.6 ± 3.3 , lidocaine 44.6 ± 3.1 ; Fig. 2). In contrast, nocebo responders reported increased pain during stimulation of the capsaicin relative to the preceding control site (control 38.7 ± 3.3 , capsaicin 56.0 ± 3.6), whereas nocebo nonresponders reported little change in pain intensity (control 42.9 ± 2.8 , capsaicin 47.8 ± 2.6).

Stimulation of the central control cream site before both the placebo and nocebo sites gave two independent preconditions to which the placebo and nocebo responses were compared. Average pain intensity ratings for all subjects between control series 1 and 2 were not significantly different (mean \pm SEM VAS: control placebo: 39.4 ± 2.3 ; control nocebo: 40.6 ± 2.3 ; $p = 0.41$; paired t test). Additionally, neither test temperature nor pain intensity ratings during stimulation of the control sites differed between responders and nonresponders for either the placebo (mean \pm SEM test temperature $^{\circ}\text{C}$: responders 47.4 ± 0.3 ; nonresponders 46.9 ± 0.2 ; $F_{(2,23)} = 0.83$, $p = 0.28$; mean \pm SEM VAS control: $F_{(2,23)} = 0.17$, $p = 0.69$) or nocebo groups (test temperature: responders 47.4 ± 0.1 ; nonresponders 46.8 ± 0.3 , $F_{(2,23)} = 3.61$, $p = 0.07$; VAS control: $F_{(2,23)} = 0.85$, $p = 0.37$). Additionally, in all subjects, there were no significant linear relationships between placebo and nocebo abilities; that is, changes in average VAS responses ($r = 0.09$, $p = 0.67$), between placebo expected and perceived pain changes ($r = 0.05$, $p = 0.81$), or nocebo expected and perceived pain changes ($r = 0.41$, $p = 0.06$).

fMRI results

Placebo analgesia

Comparison of signal intensity changes during control site versus lidocaine site stimulation in responders and nonresponders revealed that the placebo response was associated with signal intensity changes in several distinct brainstem nuclei, including the PAG and the RVM. In placebo analgesia responders, placebo-related signal intensity increases, that is, signal increases during lidocaine and decreases during control site stimulation, occurred contralateral to the stimulated forearm in the vPAG and the rostral ventrolateral medulla (RVL), ipsilateral to the stimulated forearm in the substantia nigra (SN), and on the midline in the rostral ventromedial medulla (RVM). Signal intensity in the contralateral subnucleus reticularis dorsalis (SRD) increased during lidocaine but did not change during control site stimulation. A significant placebo-analgesia-related signal decrease occurred in the region encompassing the locus coeruleus (LC) contralateral to the noxious stimulation (Fig. 3; Table 1). Compared with control site stimulation, nonresponders showed bilateral signal increases in the vPAG; however, they showed signal decreases in the RVM, in the contralateral RVL and SRD, bilaterally in the SN, and in the region of the ventral tegmental area (VTA) during lidocaine site stimulation.

Correlation analysis of signal intensity change differences between control and lidocaine scans and average change in pain intensity, that is, placebo ability, in all 25 participants revealed a similar pattern of brainstem signal changes to that of the individual responder and nonresponder groups. That is, signal intensity changes were negatively correlated with placebo ability, meaning, as placebo magnitude increased, signal change differences (lidocaine-control) were smaller in the regions of the ipsilateral dl/PAG and contralateral LC as well as in a region encompassing the

Table 1. Location, level of significance and cluster size of significant clusters in each of the placebo groups and correlation analyses

	MNI coordinates			<i>t</i> value	Cluster size ^a	Volume (mm ³)	Beta value change (mean ± SEM)	
	<i>x</i>	<i>y</i>	<i>z</i>				Control scan	Lidocaine scan
Placebo responders								
PBO > control								
Contralateral PAG	−1	−30	−6	6.33	46	5.75	−0.38 ± 0.36	1.70 ± 0.44
Ipsilateral SN	12	−27	−6	4.86	20	2.5	−0.58 ± 0.31	0.68 ± 0.35
	11	−19	−8	5.47	31	3.875		
Contralateral RVLN	−5	−38	−42	5.78	39	4.875	−0.25 ± 0.16	0.74 ± 0.26
RVM	−2	−30	−46	4.18	16	2	−1.01 ± 0.34	0.74 ± 0.26
	5	−35	−47	4.80	27	3.375		
Contralateral SRD	−2	−46	−53	4.79	13	1.625	−0.01 ± 0.13	1.07 ± 0.17
Control > PBO								
Contralateral LC	−1	−33	−18	6.32	103	12.875	1.03 ± 0.26	−0.70 ± 0.41
Placebo nonresponders								
PBO > control								
Ipsilateral PAG	3	−33	−9	3.91	17	2.125	−0.59 ± 0.22	0.79 ± 0.19
Contralateral PAG	−2	−32	−9	4.56	28	3.5	−0.15 ± 0.22	0.78 ± 0.18
Control > PBO								
Ipsilateral SN	10	−21	−6	5.91	59	7.375	1.19 ± 0.16	−0.08 ± 0.19
Contralateral SN	−12	−21	−7	4.36	45	5.625	0.82 ± 0.21	−0.32 ± 0.17
VTA	−1	−20	−6	4.80	64	8	1.01 ± 0.24	−0.21 ± 0.29
Contralateral RVLN	−6	−38	−42	4.78	123	15.375	0.87 ± 0.17	−0.22 ± 0.15
RVM	2	−31	−42	5.62	21	2.625	0.94 ± 0.28	−0.07 ± 0.24
	1	−41	−46	5.34	29	3.625		
Contralateral SRD	−1	−41	−53	3.91	29	3.625	0.74 ± 0.21	−0.27 ± 0.13
Placebo correlations								
							<i>r</i> values	
Negative correlation								
Ipsilateral PAG	2	−34	−9	4.14	54	6.75	−0.65	
Contralateral LC	−1	−36	−18	4.35	64	8	−0.61	
Ipsilateral PB	9	−42	−37	3.95	50	6.25	−0.62	
Positive correlation								
Ipsilateral SN	10	−24	−6	5.51	135	16.875	0.62	
Contralateral SN	−11	−23	−7	3.34	23	2.875	0.56	
RVM	4	−31	−42	3.54	37	4.625	0.61	
Contralateral SRD	−3	−43	−53	3.54	48	6	0.66	

Coordinates are in MNI space.

^aCluster sizes are reported in resliced 0.5 mm³ voxels.

parabrachial nucleus (PB). Conversely, signal changes positively correlated with placebo ability in the ipsilateral and contralateral SN, the RVM, and in the contralateral SRD (Figs. 3, 5; Table 1).

Nocebo hyperalgesia

Analysis of signal intensity changes associated with nocebo responses revealed similar overall patterns of brainstem changes. In nocebo hyperalgesia responders, nocebo-induced decreases (i.e., signal intensity decreased from baseline during capsaicin and increased during control site stimulation) were found bilaterally in the IPAG, in the SN contralateral to the stimulated forearm, and again on the midline in the RVM (Fig. 4; Table 2). In contrast, in nonresponders, capsaicin cream stimulation evoked signal intensity increases in the contralateral IPAG; bilaterally in the SN, RVM, and VTA; ipsilateral LC; and in the region of the nucleus cuneiformis (NCF). Additionally, a signal intensity decrease was found in the ipsilateral PB.

Correlation analysis revealed that nocebo ability was positively correlated with the change in signal between the control and capsaicin scans in the dl/IPAG and PB ipsilateral to the forearm stimulation, and bilaterally in the SN. It was negatively correlated with signal changes in the RVM and ipsilateral LC (Figs. 4, 5; Table 2).

Figure 5 shows a summary of the significant signal intensity changes correlated to placebo and nocebo ability for all 25 participants. It is clear that within the PAG and RVM, placebo and

nocebo have opposing effects. That is, greater placebo ability was associated with less PAG and greater RVM signal change, whereas greater nocebo ability was associated with greater PAG and less RVM signal change. A similar relationship was also seen in PB activity, which correlated negatively and positively with placebo and nocebo ability, respectively. In contrast, two other brainstem regions displayed similar signal relationships with both placebo and nocebo; that is, in the SN, signal changes were positively correlated and in the LC signal negatively correlated with both placebo and nocebo abilities.

PAG and RVM organization of placebo and nocebo responsiveness

Detailed analysis of the PAG revealed that apart from a group of voxels at one rostrocaudal level of the ipsilateral PAG, the vast majority of voxels that significantly correlated with placebo or nocebo abilities were located in the contralateral PAG (Fig. 6). For placebo, negatively correlated voxels were located at relatively caudal levels and primarily in the dlPAG and IPAG columns. No significantly correlated voxels were found in the vlPAG. For nocebo, the vast majority of positively correlated voxels were also located in the IPAG, although smaller numbers were also found in the remaining three columns at more rostral levels than those of placebo. With regard to the RVM, for both placebo and nocebo, significantly correlated voxels were located primarily at rostral levels in the middle

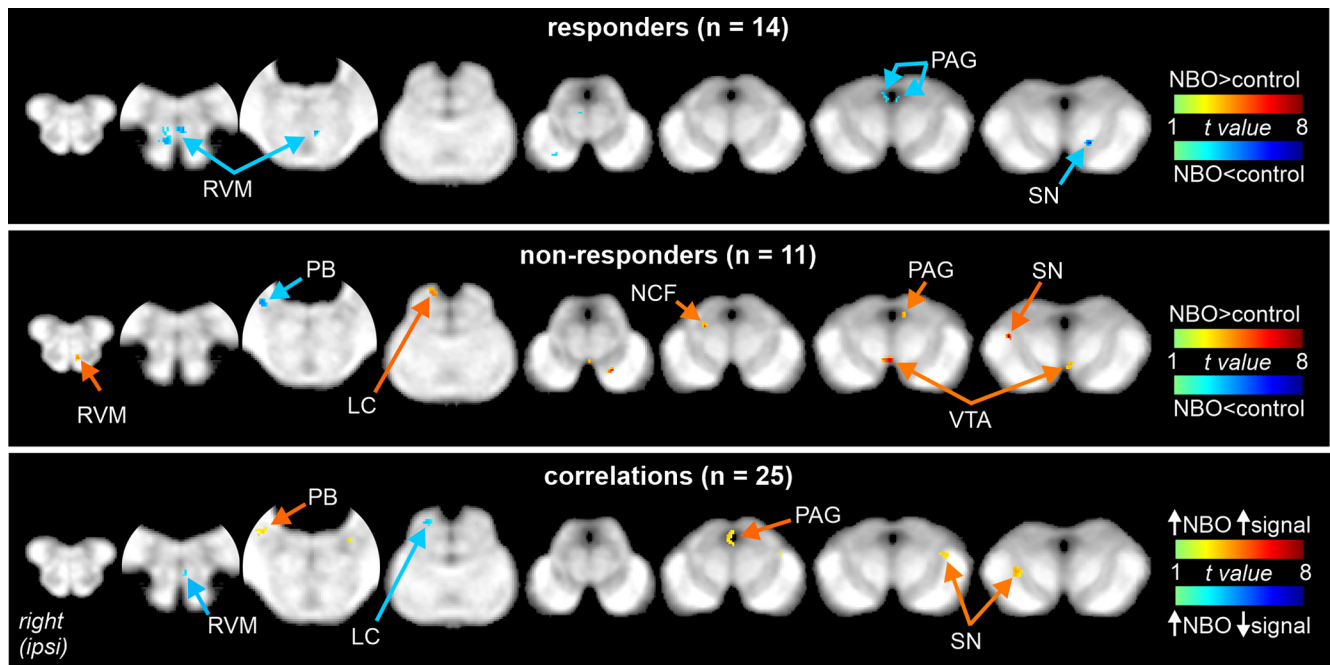


Figure 4. Signal changes in nocebo responders, nonresponders, and sites where signal change correlated with nocebo ability. Brainstem activity differed significantly between the control and capsaicin (nocebo, NBO) scans in several pain modulatory nuclei. In responders (top) signal decreases (cool color scale) occurred in the midbrain PAG bilaterally, contralateral SN, and mid-line RVM. In nonresponders (middle), signal increases (hot color scale) occurred in the contralateral PAG, the SN bilaterally, ipsilateral LC, and NCF, VTA, and RVM, and signal decreases occurred in the PB ipsilaterally. Signal intensity changes significantly correlated with nocebo ability (bottom) were found to be positively correlated (hot color scale) in the ipsilateral lateral PAG and PB, and SN bilaterally, and negatively correlated (cool color scale) in the ipsilateral LC and the RVM. PAG = periaqueductal gray, SN = substantia nigra, RVM = rostral ventromedial medulla, LC = locus coeruleus, NCF = nucleus cuneiformis, VTA = ventral tegmental area, PB = parabrachial nucleus.

and ventral aspects, although positively correlated for placebo and negatively correlated for nocebo.

Discussion

Our data reveals the first in-depth exploration of the detailed human brainstem circuitry involved in generating placebo and nocebo responses. These divergent pain modulatory responses were characterized by different activation patterns in the PAG and RVM, which together form a core brainstem pain modulatory circuit that regulates incoming noxious information at the level of the primary afferent synapse (Fields et al., 1983; Zhang et al., 1997; Fields, 2004; Tracey and Mantyh, 2007). Within the PAG, placebo and nocebo responsiveness were correlated to signal changes within the lateral and dorsolateral PAG but not within the ventrolateral PAG column. Additionally, we found that other brainstem pain modulatory sites such as the LC, PB, RVL, SRD, and SN act collectively with the PAG–RVM axis to produce both placebo and nocebo effects.

Despite the expectations of all subjects that the lidocaine and capsaicin creams would modulate pain intensity, only a proportion of individuals showed a significant change in perceived pain intensity. This is consistent with the fact that pain modulation is highly variable (Tétreault et al., 2016) as it depends on the concordance between expectation and experience (precision) of prior painful events (Grahl et al., 2018). Fewer participants responded to placebo (36%) than nocebo trials (56%), only 24% of participants responded to both nocebo and placebo, and there was no significant relationship between placebo and nocebo abilities. These proportions are similar to those reported in other investigations (Levine et al., 1979; Grevert et al., 1983; Levine and Gordon, 1984; Wager et al., 2004; Meister et al., 2020). Because perceived

pain intensities can vary within individuals to repeated presentations of the same noxious stimulus, we used the two SD threshold to define significant pain change and categorize individuals as responders and nonresponders. Investigating responders and nonresponders separately allowed us to highlight potential differences in an individual's ability to engage pain modulatory circuits.

Even with limited evidence, PAG–RVM–DH circuitry is assumed to be the final common pathway through which placebo analgesia and nocebo hyperalgesia are mediated (Bingel et al., 2006; Eippert et al., 2009; Tinnermann et al., 2017; Schafer et al., 2018). Indeed, our investigation supports that this brainstem circuit is a pivotal component in the potentiation of placebo and nocebo responses. We found opposing activity changes in this circuitry, with greater placebo ability associated with reduced signal changes in the dorsolateral and lateral PAG and increased signal changes in the RVM, and greater nocebo ability associated with increased signal changes in the dorsolateral and lateral PAG and reduced signal changes in the RVM. It is well established from experimental animal investigations that the RVM contains off and on neurons that inhibit and facilitate neurotransmission at the primary nociceptive synapse, respectively (Fields, 2004; Vanegas and Schaible, 2004; Benarroch, 2008; Heinricher et al., 2009; Ossipov et al., 2010). Activation of on cells is typically observed during prolonged exposure to noxious stimuli and leads to enhanced nociception (Morgan and Fields, 1994), whereas activation of off cells is believed to be sufficient to produce pronounced analgesia (Cheng et al., 1986; Ossipov et al., 2010). Our data suggest that when short duration stimuli are applied, reduced synaptic activity within the PAG results in an increase in the overall balance of RVM off-cell compared with on-cell firing, which in turn results in increased inhibition of incoming nociceptive drive at the dorsal horn and a placebo

Table 2. Location, level of significance and cluster size of significant clusters in each of the nocebo groups and correlation analyses

	MNI coordinates			t value	Cluster size ^a	Volume (mm ³)	Beta-value change (mean ± SEM)	
	x	y	z				Control scan	Capsaicin scan
Nocebo responders								
NBO < controls								
Ipsilateral PAG	2	−30	−4	3.85	16	2	1.25 ± 0.30	−0.84 ± 0.40
Contralateral PAG	−1	−28	−3	3.46	8	1	1.73 ± 0.41	−0.74 ± 0.46
Contralateral SN	−6	−18	−6	5.98	69	8.625	0.89 ± 0.20	−0.08 ± 0.20
RVM	4	−33	−45	5.92	186	23.25	0.72 ± 0.17	−0.33 ± 0.15
	1	−35	−43	4.37	26	3.25		
Nocebo nonresponders								
NBO > controls								
Contralateral PAG	−2	−28	−3	4.49	16	2	−0.73 ± 0.26	0.42 ± 0.35
Ipsilateral NCF	7	−28	−7	5.24	17	2.125	−0.67 ± 0.27	0.53 ± 0.31
Ipsilateral SN	15	−24	−3	7.91	43	5.375	−0.35 ± 0.22	1.02 ± 0.28
Contralateral SN	−5	−19	−12	8.50	23	2.875	−0.69 ± 0.26	0.91 ± 0.37
RVM	0	−31	−48	5.68	64	8	−0.60 ± 0.24	0.42 ± 0.15
Ipsilateral LC	5	−37	−17	4.58	57	7.125	−0.13 ± 0.20	1.22 ± 0.25
VTA	2	−19	−7	7.92	66	8.25	−1.41 ± 0.30	0.16 ± 0.24
NBO < controls								
Ipsilateral PB	12	−41	−35	4.70	57	7.125	0.33 ± 0.25	−1.13 ± 0.24
Nocebo correlations								
Negative correlation								
Ipsilateral LC	6	−35	−16	3.69	22	2.75	<i>r</i> values −0.61	
RVM	0	−36	−43	3.30	9	1.125	−0.57	
Positive correlation								
Ipsilateral PAG	2	−30	−5	3.57	63	7.875	0.57	
Ipsilateral SN	13	−21	−4	4.53	83	10.375	0.63	
Contralateral SN	−12	−26	−6	3.65	58	7.25	0.65	
Ipsilateral PB	12	−41	−34	3.53	42	5.25	0.63	

Coordinates are in MNI space.

^aCluster sizes are reported in resliced 0.5 mm³ voxels.

analgesic response, and conversely for hyperalgesic responses. The human RVM is difficult to localize anatomically as it is a large and complex structure extending through the caudal pons and a large section of the midline medulla. However, the clusters we identify as RVM are consistent with those identified previously in studies of placebo and attentional analgesia (Eippert et al., 2009; Oliva et al., 2021), suggesting that combined with the changes observed in the PAG, both these phenomena involved altered recruitment along this central pain modulatory pathway.

As placebo analgesic responses have been shown to be opioid mediated (Amanzio and Benedetti, 1999; Zubieta et al., 2005; Wager et al., 2007; Scott et al., 2008; Zhang et al., 2013), and vPAG-evoked analgesic responses are also opioid mediated (McNally et al., 2004; Loyd and Murphy, 2009), it has been hypothesized that placebo analgesic responses are likely mediated by the vPAG. However, we found that both placebo- and nocebo-related signal changes occurred in the lPAG and dIPAG but not the vPAG column. Experimental animal investigations have shown that lPAG stimulation produces a nonopioid analgesia coupled with active defensive behaviors (Bandler et al., 2000) that are mediated by brainstem circuits including via lPAG–RVM projections (Mantyh, 1983; Petrovic et al., 2004; Hohmann et al., 2005; Loyd and Murphy, 2009; Mokhtar and Singh, 2021). It appears that higher brain regions involved in conditioning and expectation recruit the lPAG and dIPAG to produce placebo and nocebo responses. Indeed, the anterior cingulate cortex and amygdala have been shown to be recruited during placebo analgesia (Tracey and Mantyh, 2007; Eippert et al., 2009; Freeman et al., 2015), and it is possible that the opioid-mediated nature of

placebo results from the actions of opioids on these regions and not the PAG.

Furthermore, because opioid-mediated antinociception is generally prolonged and not easily reversible (Atlas and Wager, 2012), it is possible that a long-lasting placebo analgesia involves persistent recruitment of opioid mechanisms at the level of the vPAG, whereas analgesia generated in response to brief acute stimuli rely on alternate mechanisms. Placebo analgesia, which is conditioned through administration of the nonsteroidal anti-inflammatory drug Ketoralac, is blocked by the cannabinoid receptor antagonist Rimonabant (Benedetti et al., 2011), and the dIPAG contains a dense concentration of CB1 cannabinoid receptors (Wilson-Poe et al., 2012), raising the possibility that this may be the neurochemical system mediating both our observed placebo and nocebo effects.

In addition to the PAG and RVM, a region encompassing the ipsilateral PB also displayed opposing signal intensity changes during placebo and nocebo responses; that is, signal changes negatively correlated with placebo ability but positively correlated with nocebo ability. Experimental animal studies have reported that the PB is a key integration site of nociceptive information, including relaying noxious inputs to higher brain areas (Loewy and Spyers, 1990; Petrovic et al., 2004) as well as providing descending modulatory influences over the PAG, RVM, and dorsal horn via the spinoparabrachial and spino-bulbo-spinal pathways, respectively (Gauriau and Bernard, 2002; Mainero et al., 2007; Roeder et al., 2016; Chen et al., 2017; Stroman et al., 2018; Bannister, 2019). Blocking the ipsilateral (to applied noxious stimuli) PB attenuates behavioral hyperalgesia in animals (Chen and Heinricher, 2019), and PB stimulation evokes aversive

behaviors in response to painful stimuli (Rodriguez et al., 2017). In addition to a role in placebo and nocebo, we have previously shown PB signal intensity changes during conditioned pain modulation analgesia, suggesting that the PB can modulate pain under a variety of paradigms (Youssef et al., 2016). Of course, because the PB also receives ascending noxious information from the dorsal horn, it is possible that changes in PB signal during placebo and nocebo reflect alterations in ascending drive because of the descending modulatory effects of the PAG–RVM on incoming noxious information at the dorsal horn (Yasui et al., 1989; Jasmin et al., 1997; Hunt and Mantyh, 2001; Gauriau and Bernard, 2002).

In contrast to the differential signal changes in the PAG, RVM, and PB, we found that signal within the LC was negatively correlated, SN positively correlated with both placebo and nocebo abilities, and VTA changes occurred in nonresponders only. The location of the LC cluster labeled in this study is consistent with the lateral extent of this nucleus as defined by Paxinos and Huang (2013) and previous human brain imaging investigations (Sclocco et al., 2016; Brooks et al., 2017). Although preclinical studies have shown that LC stimulation can produce a profound nonopioid analgesia (Hodge et al., 1983; Viisanen and Pertovaara, 2007), the LC, along with the SN and VTA, may be involved in an alternative aspect such as attentional or stimulus-response processes. Ascending dopaminergic circuitry can facilitate learning effects and encode prediction error, and phasic activity of midbrain dopamine neurons may be responsible for the expectations of future pain toward appetitive and aversive stimuli (Pauli et al., 2015; Nasser et al., 2017; Henderson et al., 2020) as well as updating them when expected rewarding or punishing responses are challenged (Schultz, 2002; Wager et al., 2006). The VTA plays a crucial role in coding unexpected responses to valanced predicted events, with unexpected rewarding events eliciting increased VTA firing and unexpected punishments decreasing VTA activity (Romo and Schultz, 1990; Jhou et al., 2009). Consistent with these findings, placebo and nocebo nonresponders demonstrated decreased and increased VTA signal, respectively, signal changes that may reflect unexpected punishment or reward. Additionally, the SN has been linked to unvalanced prediction error signal, enabling further processing of unexpected stimuli and cognitive flexibility within the cortex (Matsumoto and Hikosaka, 2009). Our results support SN as a pivotal driver for both

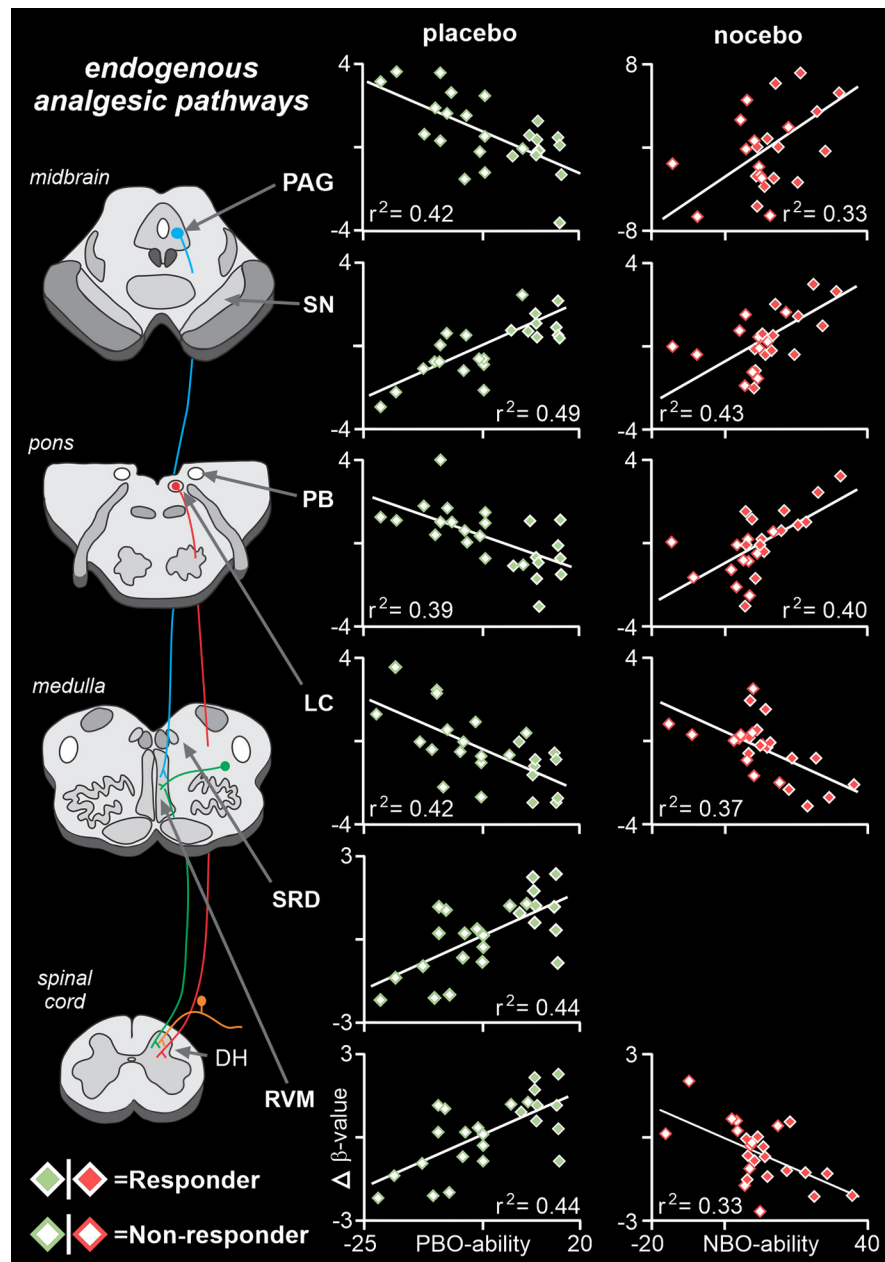


Figure 5. Divergent recruitment of brainstem sites. A summary of brainstem regions in which signal intensity changes are significantly correlated to placebo or nocebo abilities reveals that the midbrain PAG–RVM pathway displays opposing responses. That is, signal changes in the PAG are negatively correlated with placebo ability but positively correlated with nocebo ability and vice versa for the RVM. In direct contrast, brainstem regions such as the SN and LC display similar relationships with both placebo and nocebo abilities, suggesting they may be involved in aspects of placebo and nocebo that are not directly related to altering pain perception. Colored lines indicate major descending pathways within the brainstem; blue = PAG–RVM axis, green = reticular–spinal cord projections, and red = spinal projections from the LC.

positive and negative pain modulatory effects, likely through its ascending dopaminergic projections.

Finally, we found SRD and RVM signal changes associated with placebo but not nocebo. Stimulation of the PAG produces analgesic responses that are attenuated by lesions encompassing the RVM, which projects directly to the dorsal horn (Lovick, 1985; Siddall et al., 1994), and the SRD is critical in the expression of conditioned pain modulation (Youssef et al., 2016). It has been proposed that the RVM, SRD, and RVLN form an interconnected reticular triad that receives input from a variety of cortical and brainstem regions to balance nociceptive signaling (Martins and

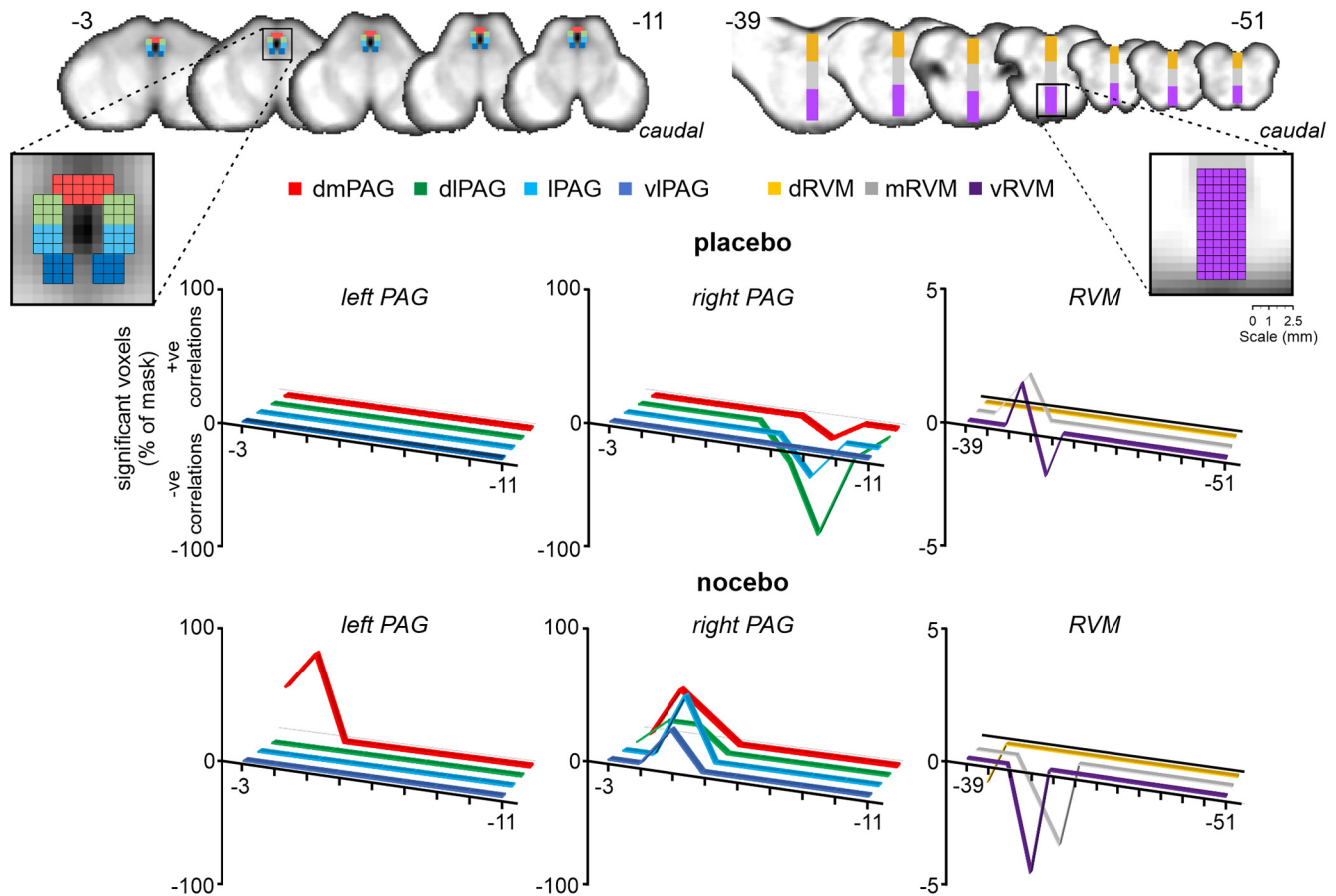


Figure 6. Regional correlations in the midbrain periaqueductal gray and rostral ventromedial medulla. Top left, Inset shows the individual masks in dmPAG (red), dlPAG (green), lPAG (light blue), and vlPAG (dark blue). Top right, Inset shows the individual masks in dRVM (orange), mRVM (gray), and vRVM (purple). The z coordinates in Montreal Neurological Institute space are indicated at the top right. Bottom, Plots depicting the percentage of voxels in each masked region that positively or negatively correlate with placebo or nocebo ability. Note that placebo and nocebo abilities are largely correlated with signal intensity changes in voxels located in discrete rostrocaudal levels of the dlPAG and lPAG as well as the middle and ventral RVM.

Tavares, 2017). Our results suggest that activation of this reticular triad underpins placebo analgesia and that when these regions are deactivated, expected analgesic effects are attenuated. Interestingly, we found only the RVM had a role in generating nocebo hyperalgesia, suggesting that placebo effects may involve a more widespread brainstem circuitry than is required for the expression of nocebo hyperalgesia.

It is important to note some limitations. First, conditioning-based models of pain modulation are prone to response bias (Hróbjartsson et al., 2011), so we asked participants to rate their pain on-line during the scan instead of afterward to reduce such potential bias. This protocol also reduced the potential for series-position effects (Murdock, 1962). Second, as the experimental design required pairing potentially modulated with nonmodulated responses, it was not possible to fully counterbalance the ordering of stimuli. We did, however, counterbalance the location and stimulation order of the lidocaine and capsaicin cream sites, reducing the likelihood of an ordering effect or location-based sensitivity. Third, although dichotomizing participants as responders and nonresponders was important for evaluating individual variations in brainstem recruitment, this may have introduced a selection bias that could influence the overall interpretation. Although the 2 SD band method constrains group assignment to individual pain responses on the same dermatome, it could be interpreted that participants with lesser pain sensitivity on the placebo-treated site would be more likely to be placebo responders and the inverse for nocebo responders. If so,

an alternative interpretation could be that the PAG–RVM circuit and the PB were responsive to the intensity of noxious stimuli rather than the manifestation of modulatory phenomena. By extension, habituation and sensitization effects to heat pain are both spatially and temporally dependent (Jepma et al., 2014). We found that pain responses for all subjects between control series 1 and 2 were not significantly different, suggesting that habituation and/or sensitization was absent during the test phase. Furthermore, although we included a 24 h period between conditioning and reinforcement, at least a 15 min period between reinforcement and test phases, and reinforcement and test phases were conducted on opposite forearms, some stimulus history effects may have remained. Fourth, we used an initial threshold of $p < 0.005$ uncorrected for multiple comparisons with a cluster extent threshold of five contiguous voxels. Our results were largely limited to brainstem nuclei previously stated to play a functional role in pain modulation, and we further performed cluster-level thresholding to reduce the potential for type 2 errors. Given that the wealth of experimental animal investigations into the brainstem sites responsible for pain modulation have identified the PAG–RVM–DH as the critical circuit, one might have hypothesized that areas such as the SRD, PB, LC, and NCF play somewhat more minor roles. However, our data do not show this with regard to overall significance, although the precise role of each of these regions in placebo and nocebo responses remains to be ascertained. Finally, although the enhanced spatial resolution provided by 7 tesla imaging allowed us to describe voxel

peaks within anatomically meaningful areas using the brainstem atlas from Paxinos and Huang (2013), we appreciate that even with increased spatial resolution we are not able to precisely identify small brainstem nuclei. Given this, the described cluster locations need to be appreciated with some caution.

Conclusions

Using ultra-high-field fMRI, we have shown, for the first time, that specific nuclei within the brainstem mediate changes in the perceived intensity of noxious stimuli to produce placebo and nocebo responses. In support of prevailing models asserting the PAG–RVM axis as the central pathway for descending pain modulatory effects, we have shown that the rostral ventromedial medulla is positively related and the periaqueductal gray inversely related to the placebo response, whereas the reverse is true for nocebo responses. We further suggest that this central circuitry alone is not solely responsible for subsequent pain modulation, but rather a more widespread engagement of pathways involving the parabrachial complex, locus ceruleus, and substantia nigra are pivotal drivers in producing significant antinociceptive and pro-nociceptive effects. The specific roles and cortical connectivity profiles of each of these brainstem regions in modulating perceived pain intensity remains to be determined and would be a valuable future investigation if we are to fully understand these complex phenomena.

References

- Amanzio M, Benedetti F (1999) Neuropharmacological dissection of placebo analgesia: expectation-activated opioid systems versus conditioning-activated specific subsystems. *J Neurosci* 19:484–494.
- Atlas LY, Wager TD (2012) How expectations shape pain. *Neurosci Lett* 520:140–148.
- Babel P, Adamczyk W, Swider K, Bajcar EA, Kicman P, Lisinska N (2018) How classical conditioning shapes placebo analgesia: hidden versus open conditioning. *Pain Med* 19:1156–1169.
- Bandler R, Shipley MT (1994) Columnar organization in the midbrain periaqueductal gray: modules for emotional expression? *Trends Neurosci* 17:379–389.
- Bandler R, Keay KA (1996) Columnar organization in the midbrain periaqueductal gray and the integration of emotional expression. *Prog Brain Res* 107:285–300.
- Bandler R, Keay KA, Floyd N, Price J (2000) Central circuits mediating patterned autonomic activity during active vs. passive emotional coping. *Brain Res Bull* 53:95–104.
- Bannister K (2019) Descending pain modulation: influence and impact. *Curr Opin Physiol* 11:62–66.
- Benarroch EE (2008) Descending monoaminergic pain modulation: bidirectional control and clinical relevance. *Neurology* 71:217–221.
- Benedetti F, Amanzio M, Rosato R, Blanchard C (2011) Nonopioid placebo analgesia is mediated by CB1 cannabinoid receptors. *Nat Med* 17:1228–1230.
- Bingel U, Lorenz J, Schoell E, Weiller C, Büchel C (2006) Mechanisms of placebo analgesia: rACC recruitment of a subcortical antinociceptive network. *Pain* 120:8–15.
- Brooks JCW, Davies W-E, Pickering AE (2017) Resolving the brainstem contributions to attentional analgesia. *J Neurosci* 37:2279–2291.
- Chen Q, Heinricher MM (2019) Plasticity in the link between pain-transmitting and pain-modulating systems in acute and persistent inflammation. *J Neurosci* 39:2065–2079.
- Chen Q, Roeder Z, Li MH, Zhang Y, Ingram SL, Heinricher MM (2017) Optogenetic evidence for a direct circuit linking nociceptive transmission through the parabrachial complex with pain-modulating neurons of the rostral ventromedial medulla (RVM). *eNeuro* 4:ENEURO.0202-17.2017.
- Cheng ZF, Fields HL, Heinricher MM (1986) Morphine microinjected into the periaqueductal gray has differential effects on 3 classes of medullary neurons. *Brain Res* 375:57–65.
- Coulombe MA, Erpelding N, Kucyi A, Davis KD (2016) Intrinsic functional connectivity of periaqueductal gray subregions in humans. *Hum Brain Mapp* 37:1514–1530.
- Craggs JG, Price DD, Verne GN, Perlstein WM, Robinson MM (2007) Functional brain interactions that serve cognitive-affective processing during pain and placebo analgesia. *Neuroimage* 38:720–729.
- Diedrichsen J (2006) A spatially unbiased atlas template of the human cerebellum. *Neuroimage* 33:127–138.
- Egorova N, Benedetti F, Gollub RL, Kong J (2019) Between placebo and nocebo: response to control treatment is mediated by amygdala activity and connectivity. *Eur J Pain* 24:580–592.
- Eippert F, Bingel U, Schoell ED, Yacubian J, Klinger R, Lorenz J, Büchel C (2009) Activation of the opioidergic descending pain control system underlies placebo analgesia. *Neuron* 63:533–543.
- Faul F, Erdfelder E, Lang AG, Buchner A (2007) G*Power 3: a flexible statistical power analysis program for the social, behavioral, and biomedical sciences. *Behav Res Methods* 39:175–191.
- Faull OK, Jenkinson M, Clare S, Pattinson KTS (2015) Functional subdivision of the human periaqueductal grey in respiratory control using 7 tesla fMRI. *Neuroimage* 113:356–364.
- Fields H (2004) State-dependent opioid control of pain. *Nat Rev Neurosci* 5:565–575.
- Fields HL, Bry J, Hentall I, Zorman G (1983) The activity of neurons in the rostral medulla of the rat during withdrawal from noxious heat. *J Neurosci* 3:2545–2552.
- Finniss DG, Kaptchuk TJ, Miller F, Benedetti F (2010) Biological, clinical, and ethical advances of placebo effects. *The Lancet* 375:686–695.
- Freeman S, Yu R, Egorova N, Chen X, Kirsch I, Claggett B, Kaptchuk TJ, Gollub RL, Kong J (2015) Distinct neural representations of placebo and nocebo effects. *Neuroimage* 112:197–207.
- Frisaldi E, Piedimonte A, Benedetti F (2015) Placebo and nocebo effects: a complex interplay between psychological factors and neurochemical networks. *Am J Clin Hypn* 57:267–284.
- Gauriau C, Bernard JF (2002) Pain pathways and parabrachial circuits in the rat. *Exp Physiol* 87:251–258.
- Grahl A, Onat S, Büchel C (2018) The periaqueductal gray and Bayesian integration in placebo analgesia. *Elife* 7:e32930.
- Grevert P, Albert LH, Goldstein A (1983) Partial antagonism of placebo analgesia by naloxone. *Pain* 16:129–143.
- Hansen E, Zech N, Meissner K (2017) [Placebo and nocebo: how can they be used or avoided? *Internist (Berl)* 58:1102–1110.
- Heinricher MM, Tavares I, Leith JL, Lumb BM (2009) Descending control of nociception: specificity, recruitment and plasticity. *Brain Res Rev* 60:214–225.
- Henderson LA, Di Pietro F, Youssef AM, Lee S, Tam S, Akhter R, Mills EP, Murray GM, Peck CC, Macey PM (2020) Effect of expectation on pain processing: a psychophysics and functional MRI analysis. *Front Neurosci* 14:6–6.
- Hibi D, Takamoto K, Iwama Y, Ebina S, Nishimaru H, Matsumoto J, Takamura Y, Yamazaki M, Nishijo H (2020) Impaired hemodynamic activity in the right dorsolateral prefrontal cortex is associated with impairment of placebo analgesia and clinical symptoms in postherpetic neuralgia. *IBRO Rep* 8:56–64.
- Hodge CJ, Apkarian AV, Owen MP, Hanson BS (1983) Changes in the effects of stimulation of locus coeruleus and nucleus raphe magnus following dorsal rhizotomy. *Brain Res* 288:325–329.
- Hohmann AG, Suplita RL, Bolton NM, Neely MH, Fegley D, Mangieri R, Krey JF, Walker JM, Holmes PV, Crystal JD, Duranti A, Tontini A, Mor M, Tarzia G, Piomelli D (2005) An endocannabinoid mechanism for stress-induced analgesia. *Nature* 435:1108–1112.
- Hróbjartsson A, Kaptchuk TJ, Miller FG (2011) Placebo effect studies are susceptible to response bias and to other types of biases. *J Clin Epidemiol* 64:1223–1229.
- Hunt SP, Mantyh PW (2001) The molecular dynamics of pain control. *Nat Rev Neurosci* 2:83–91.
- Jasmin L, Burkey AR, Card JP, Basbaum AI (1997) Transneuronal labeling of a nociceptive pathway, the spino-(trigemino-)parabrachio-amygdaloid, in the rat. *J Neurosci* 17:3751–3765.
- Jepma M, Jones M, Wager TD (2014) The dynamics of pain: evidence for simultaneous site-specific habituation and site-nonspecific sensitization in thermal pain. *J Pain* 15:734–746.

- Jhou TC, Geisler S, Marinelli M, Degarmo BA, Zahm DS (2009) The mesopontine rostromedial tegmental nucleus: a structure targeted by the lateral habenula that projects to the ventral tegmental area of Tsai and substantia nigra compacta. *J Comp Neurol* 513:566–596.
- Kirsch J, Kong J, Sadler P, Spaeth R, Cook A, Kaptchuk T, Gollub R (2014) Expectancy and conditioning in placebo analgesia: separate or connected processes? *Psychol Conscious (Wash D C)* 1:51–59.
- Kragel PA, Bianciardi M, Hartley L, Matthewson G, Choi J-K, Quigley KS, Wald LL, Wager TD, Feldman Barrett L, Satpute AB (2019) Functional involvement of human periaqueductal gray and other midbrain nuclei in cognitive control. *J Neurosci* 39:6180–6189.
- Levine JD, Gordon NC (1984) Influence of the method of drug administration on analgesic response. *Nature* 312:755–756.
- Levine JD, Gordon NC, Bornstein JC, Fields HL (1979) Role of pain in placebo analgesia. *Proc Natl Acad Sci U S A* 76:3528–3531.
- Linnman C, Moulton EA, Barmettler G, Becerra L, Borsook D (2012) Neuroimaging of the periaqueductal gray: state of the field. *Neuroimage* 60:505–522.
- Loewy AD, Spyer KM (1990) Vagal preganglionic neurons. In: *Central regulation of Autonomic Functions* (Loewy AD, Spyer KM eds), pp 68–87. New York: Oxford University Press.
- Lovick TA (1985) Ventrolateral medullary lesions block the antinociceptive and cardiovascular responses elicited by stimulating the dorsal periaqueductal grey matter in rats. *Pain* 21:241–252.
- Loyd DR, Murphy AZ (2009) The role of the periaqueductal gray in the modulation of pain in males and females: are the anatomy and physiology really that different? *Neural Plast* 2009:462879.
- Mainiero C, Zhang W-T, Kumar A, Rosen BR, Sorensen AG (2007) Mapping the spinal and supraspinal pathways of dynamic mechanical allodynia in the human trigeminal system using cardiac-gated fMRI. *Neuroimage* 35:1201–1210.
- Mantyh PW (1983) Connections of midbrain periaqueductal gray in the monkey. II. Descending efferent projections. *J Neurophysiol* 49:582–594.
- Martins I, Tavares I (2017) Reticular formation and pain: the past and the future. *Front Neuroanat* 11:51.
- Matsumoto M, Hikosaka O (2009) Two types of dopamine neuron distinctly convey positive and negative motivational signals. *Nature* 459:837–841.
- McNally GP, Pigg M, Weidemann G (2004) Opioid Receptors in the midbrain periaqueductal gray regulate extinction of pavlovian fear conditioning. *J Neurosci* 24:6912–6919.
- Medoff ZM, Colloca L (2015) Placebo analgesia: understanding the mechanisms. *Pain Manag* 5:89–96.
- Meister R, Abbas M, Antel J, Peters T, Pan Y, Bingel U, Nestorciuc Y, Hebebrand J (2020) Placebo response rates and potential modifiers in double-blind randomized controlled trials of second and newer generation antidepressants for major depressive disorder in children and adolescents: a systematic review and meta-regression analysis. *Eur Child Adolesc Psychiatry* 29:253–273.
- Mokhtar M, Singh P (2021) Neuroanatomy, periaqueductal gray. Treasure Island, FL: StatPearls.
- Morgan MM, Fields HL (1994) Pronounced changes in the activity of nociceptive modulatory neurons in the rostral ventromedial medulla in response to prolonged thermal noxious stimuli. *J Neurophysiol* 72:1161–1170.
- Murdock BB Jr (1962) The serial position effect of free recall. *J Exp Psychol* 64:482–488.
- Nasser HM, Calu DJ, Schoenbaum G, Sharpe MJ (2017) The dopamine prediction error: contributions to associative models of reward learning. *Front Psychol* 8:244–244.
- Oliva V, Gregory R, Davies W-E, Harrison L, Moran R, Pickering AE, Brooks JCW (2021) Parallel cortical-brainstem pathways to attentional analgesia. *Neuroimage* 226:117548.
- Ossipov MH, Dussor GO, Porreca F (2010) Central modulation of pain. *J Clin Invest* 120:3779–3787.
- Palazzo E, Luongo L, de Novellis V, Rossi F, Maione S (2010) The role of cannabinoid receptors in the descending modulation of pain. *Pharmaceuticals (Basel)* 3:2661–2673.
- Pauli WM, Larsen T, Collette S, Tyszka JM, Seymour B, O'Doherty JP (2015) Distinct contributions of ventromedial and dorsolateral subregions of the human substantia nigra to appetitive and aversive learning. *J Neurosci* 35:14220–14233.
- Paxinos G, Huang X-F (2013) Atlas of the human brainstem. Burlington, VT: Elsevier Science.
- Penny WD, Friston KJ, Ashburner JT, Kiebel SJ, Nichols TE (2011) Statistical parametric mapping: the analysis of functional brain images. Amsterdam, Netherlands: Elsevier.
- Petrovic P, Kalso E, Petersson KM, Ingvar M (2002) Placebo and opioid analgesia—imaging a shared neuronal network. *Science* 295:1737–1740.
- Petrovic P, Petersson KM, Hansson P, Ingvar M (2004) Brainstem involvement in the initial response to pain. *Neuroimage* 22:995–1005.
- Rodriguez E, Sakurai K, Xu J, Chen Y, Toda K, Zhao S, Han BX, Ryu D, Yin H, Liedtke W, Wang F (2017) A craniofacial-specific monosynaptic circuit enables heightened affective pain. *Nat Neurosci* 20:1734–1743.
- Roeder Z, Chen Q, Davis S, Carlson JD, Tupone D, Heinricher MM (2016) Parabrachial complex links pain transmission to descending pain modulation. *Pain* 157:2697–2708.
- Romo R, Schultz W (1990) Dopamine neurons of the monkey midbrain: contingencies of responses to active touch during self-initiated arm movements. *J Neurophysiol* 63:592–606.
- Särkkä S, Solin A, Nummenmaa A, Vehtari A, Auranen T, Vanni S, Lin F-H (2012) Dynamic retrospective filtering of physiological noise in BOLD fMRI: DRIFTER. *NeuroImage* 60:1517–1527.
- Satpute AB, Wager TD, Cohen-Adad J, Bianciardi M, Choi JK, Buhle JT, Wald LL, Barrett LF (2013) Identification of discrete functional subregions of the human periaqueductal gray. *Proc Natl Acad Sci U S A* 110:17101–17106.
- Schafer SM, Geuter S, Wager TD (2018) Mechanisms of placebo analgesia: a dual-process model informed by insights from cross-species comparisons. *Prog Neurobiol* 160:101–122.
- Schenk LA, Colloca L (2020) The neural processes of acquiring placebo effects through observation. *Neuroimage* 209:116510.
- Schielen A, Höfler C, Übel S, Wabnegger A (2018) Emotion-specific nocebo effects: an fMRI study. *Brain Imaging Behav* 12:180–187.
- Schultz W (2002) Getting formal with dopamine and reward. *Neuron* 36:241–263.
- Sclocco R, Beissner F, Desbordes G, Polimeni JR, Wald LL, Kettner NW, Kim J, Garcia RG, Renvall V, Bianchi AM, Cerutti S, Napadow V, Barbieri R (2016) Neuroimaging brainstem circuitry supporting cardiovascular response to pain: a combined heart rate variability/ultrahigh-field (7 T) functional magnetic resonance imaging study. *Phil Trans R Soc A* 374:20150189.
- Sclocco R, Beissner F, Bianciardi M, Polimeni JR, Napadow V (2018) Challenges and opportunities for brainstem neuroimaging with ultrahigh field MRI. *NeuroImage* 168:412–426.
- Scott DJ, Stohler CS, Egnatuk CM, Wang H, Koeppel RA, Zubieta JK (2008) Placebo and nocebo effects are defined by opposite opioid and dopaminergic responses. *Arch Gen Psychiatry* 65:220–231.
- Sevel LS, Craggs JG, Price DD, Staud R, Robinson ME (2015) Placebo analgesia enhances descending pain-related effective connectivity: a dynamic causal modeling study of endogenous pain modulation. *J Pain* 16:760–768.
- Siddall PJ, Polson JW, Dampney RAL (1994) Descending antinociceptive pathway from the rostral ventrolateral medulla: a correlative anatomical and physiological study. *Brain Res* 645:61–68.
- Sims-Williams H, Matthews JC, Talbot PS, Love-Jones S, Brooks JC, Patel NK, Pickering AE (2017) Deep brain stimulation of the periaqueductal gray releases endogenous opioids in humans. *NeuroImage* 146:833–842.
- Stroman PW, Joachim G, Powers JM, Staud R, Pukall C (2018) Pain processing in the human brainstem and spinal cord before, during, and after the application of noxious heat stimuli. *Pain* 159:2012–2020.
- Tétreault P, Mansour A, Vachon-Pressseau E, Schnitzer TJ, Apkarian AV, Baliki MN (2016) Brain connectivity predicts placebo response across chronic pain clinical trials. *PLOS Biol* 14:e1002570.
- Tinnermann A, Geuter S, Sprenger C, Finsterbusch J, Büchel C (2017) Interactions between brain and spinal cord mediate value effects in nocebo hyperalgesia. *Science* 358:105–108.
- Tracey I, Mantyh PW (2007) The cerebral signature for pain perception and its modulation. *Neuron* 55:377–391.
- Vanegas H, Schaible HG (2004) Descending control of persistent pain: inhibitory or facilitatory? *Brain Res Brain Res Rev* 46:295–309.
- Vase L, Robinson ME, Verne GN, Price DD (2005) Increased placebo analgesia over time in irritable bowel syndrome (IBS) patients is associated with

- desire and expectation but not endogenous opioid mechanisms. *Pain* 115:338–347.
- Viisanen H, Pertovaara A (2007) Influence of peripheral nerve injury on response properties of locus coeruleus neurons and coeruleospinal antinociception in the rat. *Neuroscience* 146:1785–1794.
- Voudouris NJ, Peck CL, Coleman G (1989) Conditioned response models of placebo phenomena: further support. *Pain* 38:109–116.
- Voudouris NJ, Peck CL, Coleman G (1990) The role of conditioning and verbal expectancy in the placebo response. *Pain* 43:121–128.
- Wager TD, Rilling JK, Smith EE, Sokolik A, Casey KL, Davidson RJ, Kosslyn SM, Rose RM, Cohen JD (2004) Placebo-induced changes in FMRI in the anticipation and experience of pain. *Science* 303:1162–1167.
- Wager TD, Matre D, Casey KL (2006) Placebo effects in laser-evoked pain potentials. *Brain Behav Immun* 20:219–230.
- Wager TD, Scott DJ, Zubieta JK (2007) Placebo effects on human mu-opioid activity during pain. *Proc Natl Acad Sci U S A* 104:11056–11061.
- Wilson-Poe AR, Morgan MM, Aicher SA, Hegarty DM (2012) Distribution of CB1 cannabinoid receptors and their relationship with mu-opioid receptors in the rat periaqueductal gray. *Neuroscience* 213:191–200.
- Yasui Y, Saper CB, Cechetto DF (1989) Calcitonin gene-related peptide immunoreactivity in the visceral sensory cortex, thalamus, and related pathways in the rat. *J Comp Neurol* 290:487–501.
- Youssef AM, Macefield VG, Henderson LA (2016) Pain inhibits pain; human brainstem mechanisms. *Neuroimage* 124:54–62.
- Zhang C, Yang SW, Guo YG, Qiao JT, Dafny N (1997) Locus coeruleus stimulation modulates the nociceptive response in parafascicular neurons: an analysis of descending and ascending pathways. *Brain Res Bull* 42:273–278.
- Zhang R-R, Zhang W-C, Wang J-Y, Guo J-Y (2013) The opioid placebo analgesia is mediated exclusively through μ -opioid receptor in rat. *Int J Neuropsychopharmacol* 16:849–856.
- Zubieta J-K, Bueller JA, Jackson LR, Scott DJ, Xu Y, Koeppe RA, Nichols TE, Stohler CS (2005) Placebo effects mediated by endogenous opioid activity on μ -opioid receptors. *J Neurosci* 25:7754–7762.